

International Journal of INTELLIGENT SYSTEMS AND APPLICATIONS IN ENGINEERING

ISSN:2147-6799 www.ijisae.org Original Research Paper

Enhancing Space Coverage Area for Cellular Communication Systems via 3D-IRS

Abdulmajeed S. Alaqeel¹, Anwar Hassan Ibrahim²

Submitted: 15/03/2024 Revised: 29/04/2024 Accepted: 06/05/2024

Abstract: Currently, most of the research direction goal is to ascertain the impact of a full space coverage enhancement for cellular communication systems. The objective of this paper is to enhancing the space coverage of contemporary cellular communication systems in accordance to the ordinary single Intelligent Reflective Surfaces (S-IRS) Algorithm. MATLAB software has been used to implement the three-dimensional intelligent reflective surface (3D-IRS) technique in order to optimize the wireless coverage in a certain region. The Coverage Maximization Algorithm (CMA) with the same parameters has been demonstrated to show the proposed 3D-IRS which was developed in a well-structured manner to obtain a good margin. The results show that the performance of the system was increased by 16.61% with respect to the singular IRS and shows the leap in aspect of area of spatial horizon measured by squared meters. This application optimizes with a BS power of 2 Watts, the threshold distance increased by 39 meters, while the coverage area expanded by 132520 m². Two IRSs deployments yielded even more coverage of 1583500 m² when applying for the IRSs full integration. In conclusion the entire capacity of 3D-IRS's complete spatial capability, and demonstrated the stability of different IRS settings. Furthermore, the analysis of RSSI indicated that 3D-IRS maintained superior signal quality over increased distances, particularly influenced by the number of reflective elements and the base station transmitting power.

Keywords: Full Space, Coverage, Intelligent Reflective Surfaces, Reconfigurable Intelligent Surface, 5G, 6G, mmWave, THz, Mobile Communication

1. Introduction

The Intelligent Reflecting Surface has emerged as a groundbreaking and transformative technique that fundamentally alters the landscape of radio propagation environments by dynamically and adaptively adjusting various wireless signal parameters, which include but are not limited to amplitude and phase, through the utilization of controllable reflecting components designed for optimal performance [1]. In stark contrast to traditional solutions employed in the industry, the IRS technology leverages low-cost and passive reflecting meta-surfaces that are capable of significantly altering critical signal attributes such as frequency, polarization, amplitude, and phase with remarkable precision and efficiency [2], [3]. This innovative method not only proves to be feasible and economically advantageous, but it also aligns seamlessly with the imperative of environmental sustainability, thereby addressing the increasingly complex and evolving demands of contemporary wireless technologies. The operation of IRS is characterized by its functioning as a planar array consisting of numerous passive components, each of which plays a crucial role in inducing specific phase shifts in incoming electromagnetic waves, all orchestrated through an advanced and intelligent control

Department of Electrical Engineering – College of Engineering – Qassim University – 51452, KSA ORCID ID: 0000-0003-1771-6868 Corresponding Author Email: 1411100392@qu.edu.sa

system designed for optimal signal processing. The passive reflecting surfaces utilized in conventional reflect arrays have a multitude of applications within the domain of wireless communication, a fact that is vividly exemplified in the illustrative representation found in Figure 1 [4].

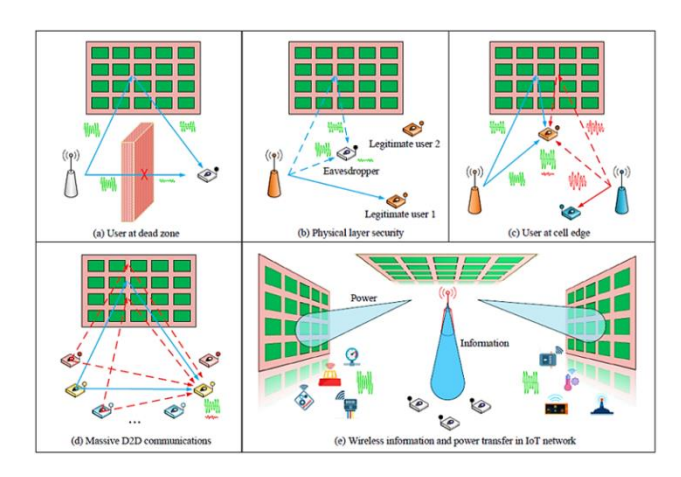


Figure 1 Applications of IRS in Wireless Communication [4]

Traditional Intelligent Reflecting Surfaces face two primary limitations that reduce their effectiveness in practical applications. Firstly, conventional IRS only modulate the phase of incident signals, which restricts the capacity of passive beamforming techniques and leads to diminished overall system performance. Secondly, these systems are limited in their operational range, as they primarily reflect signals in a single directional orientation, as established in previous studies [5].

The IRS network model is based on scattering parameters, conceptualizing an S-element IRS as an S-port reconfigurable impedance network with corresponding antennas. The scattering matrix (SM) characterizes the interaction between incident and reflected waves, providing a comprehensive representation of the network's behaviour [6].

Traditional IRS generates a diagonal SM, while more advanced three-dimensional IRS (3D-IRS) allows interconnections between ports, enhancing functionality. Uniform Linear Arrays (ULA) and Uniform Rectangular Arrays (URA) offer distinct configurations for electromagnetic wave control. ULA, a simpler onedimensional design, excels in environments requiring directional control, but its performance diminishes in complex settings with obstructions. In contrast, URA's two-dimensional arrangement allows more versatile beamforming across multiple planes, making it more suitable for advanced IRS deployments in challenging environments.

IRS, also known as Reconfigurable Intelligent Surface (RIS), consists of artificial planar structures with meta-surfaces that dynamically manipulate electromagnetic waves, significantly enhancing wireless communication by improving signal coverage, energy efficiency, and interference mitigation [7].

IRS technology can manipulate critical signal parameters such as amplitude, phase, and polarization, allowing unprecedented control over wireless communication channels. Recent research has classified IRS based on passive or active characteristics, with passive surfaces manipulating signals without additional energy and active surfaces integrating energy sources for advanced signal processing [8], [9]. Another classification distinguishes between discrete and continuous IRS, where discrete surfaces have individually controllable elements, and continuous surfaces provide seamless control of the electromagnetic field [10], [11]. Figure 2 illustrates examples of electromagnetic (EM)-based elementary functions used by IRS, highlighting their potential applications in wireless communication systems.

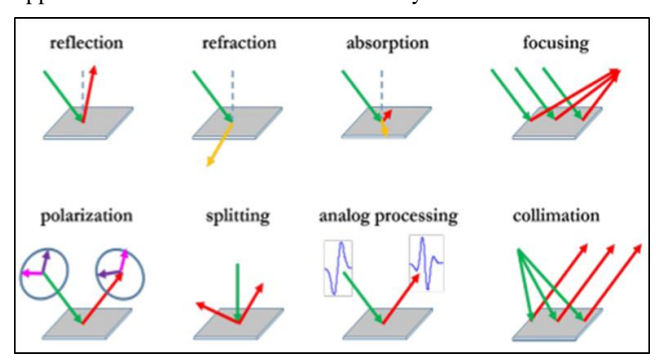


Figure 2 Elementary functions of IRS based on EM principles

2. Related Work

Intelligent Reflecting Surfaces (IRS) are two-dimensional planes composed of numerous passive reflecting elements, each capable of independently manipulating either the amplitude or phase of incoming signals in a controlled manner. The strategic deployment of IRSs in wireless communication networks facilitates the reorganization of wireless channels and signal propagation pathways between transmitters and receivers. This innovative approach effectively addresses challenges posed by interference and fading in wireless channels, significantly enhancing the capacity and reliability of communication systems. These advancements not only improve performance metrics but also contribute to the evolution of communication paradigms in our interconnected world. Research has extensively examined rapid beam training methodologies for millimetre-wave cellular systems incorporating IRS technology, marking a pioneering contribution to the field [12]. This work explores an expedited beam training technique aimed at optimizing beam pairings among the Base Station (BS), IRS, and Mobile Station (MS) within millimetrewave (mmWave) systems utilizing IRS. The work in previous paper proposed method employs a uniform rectangular array (URA) at each critical location BS, IRS, and MS to facilitate mmWave beamforming operations, conceptualizing this arrangement as regular linear arrays (ULAs). The BS's URA is partitioned into distinct ULAs, allowing concurrent beam transmission across various directions. The IRS reflects incoming signals diversely to enhance communication efficacy. In environments with multiple beam receptions, the MS must efficiently discern its cell ID (CID) and beam ID (BID) from received signals, subsequently correlating them with reference Base Transceiver Stations (BTSs) to identify optimal beam pairings (BS↔IRS↔MS).

While there is considerable academic enthusiasm for IRS as solutions to mmWave and THz coverage gaps, many studies rely on assumptions unlikely to hold in real deployments. A significant amount of work examines IRS based on optimal communication channels between the IRS and base stations [13]. The proposed 3D-IRS concept is inspired by the dynamic meta surface antennas (DMAs) [14], [15], which, compared to standard multiple-input multiple-output (MIMO) arrays, offer a potential technique for expanding antenna components at lower costs and with efficient power consumption. Early IRS control circuitry prototypes exhibit non-negligible phase-shift reconfiguration times maintaining low power consumption (in the hundreds of mW range) [16]. Additionally, research indicates a proportional relationship between the number of sectoral antennas and throughput (bps), as described in reference [17], where a multisector is defined as a network of reconfigurable impedance ports linked by multiple antennas. Antennas structured as 3D-IRS have to have sectors greater than one. Developing precise metrics and models to measure IRS-induced coverage improvements poses significant challenges due to the need for real-time considerations of coverage requirements and environmental factors influencing signal behaviour. The dynamic nature of wireless networks necessitates real-time reconfiguration of IRS units, introducing hardware and algorithmic complexities. Determining optimal IRS placement to extend coverage without increasing interference is particularly complex in multi-user scenarios, requiring a balance between coverage and capacity improvements. Integrating IRS technology with emerging advancements such as millimetre wave (mmWave) and Terahertz communications further complicates

Ensuring consistent service quality in challenging environments, such as cell edges, indoor spaces, and underground locations, remains a critical challenge. Seamless handover strategies in IRSassisted networks and reliable coverage prediction models accounting for IRS impacts necessitate further research. Addressing these challenges is essential for maximizing the potential of IRS in next-generation networks. Solutions must balance innovation with practical concerns, including cost efficiency, energy use, and regulatory compliance. As research progresses, overcoming these issues will be vital for achieving widespread improvements in cellular network coverage through IRS technology.

3. Proposed Method

The overarching methodology that underpins this research endeavour is fundamentally anchored in a vast array of preceding scholarly inquiries, encompassing a diverse collection of academic papers and journals, which, regrettably, have largely overlooked the pivotal significance of ensuring comprehensive spatial coverage, a critical aspect that has been previously discussed in detail within this thesis. Rather than prioritizing this essential element, the predominant attention of these earlier works has been disproportionately allocated to a multitude of other factors, which, while undeniably important, such as the intricacies surrounding power consumption, the precise alignment of beams, the meticulous sizing of IRS antenna elements, and the employment of various forms of unmanned aerial vehicles (UAVs), which must not be misconstrued, as these topics are indeed of great relevance and merit thorough investigation and analysis.

This scholarly work elucidates a ground-breaking technological advancement aimed at achieving comprehensive spatial coverage through the implementation of a three-dimensional intelligent reflecting surface (3D-IRS).

Moreover, the optimization of the multiple planner 3D-IRS system holds the potential to significantly enhance its operational efficacy, which in turn assists in mitigating the requirement for a dedicated spatial zone. Nevertheless, it must be noted that the implementation of the 3D-IRS is fundamentally geared towards augmenting the overall efficiency and performance of effective IRS models, rendering them superior in comparison to the earlier research efforts that have been introduced within this specific domain of study.

To facilitate a thorough empirical investigation, the initial conceptual framework of the 3D-IRS is meticulously examined in conjunction with three-dimensional modelling software, as depicted in the illustrative representation provided in figure 3 below:

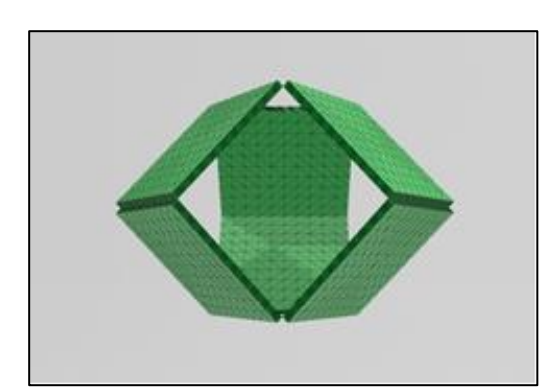


Figure 3 Initial Concept of 3D-IRS with 6 Sectors

In advancing the comprehensive implementation of the threedimensional intelligent reflecting surface (3D-IRS) network, particularly regarding intricate arithmetic calculations and coding procedures using advanced programming tools like MATLAB and sophisticated 3D emulators, there is a pressing need for an academic revaluation of the initial design approach. The shift from utilizing six sectorial planes to a configuration of three sectorial planes offers considerable research advantages that warrant attention.

The primary justifications for adopting a three-sectoral plane design over the initial six-sectoral plane design, are summarized as follows:

1. Adequate Coverage: A three-sectoral plane 3D-IRS is sufficient to provide comprehensive coverage across the entire cellular space,

ensuring optimal signal distribution and user connectivity.

- 2. Reduced Power Consumption: Operating a six-sectoral plane 3D-IRS would lead to significantly higher power consumption, potentially compromising overall system performance and sustainability.
- 3. Space Requirements: The physical space needed for deploying a six-sectoral plane system would be larger, requiring a greater volumetric footprint for both the 3D-IRS hardware and its control mechanisms, complicating installation and integration.
- 4. Increased Weight: A six-sectoral plane configuration would proportionally increase the system's weight, posing structural support and stability challenges for the implemented infrastructure.
- 5. Limited Need for Upper Coverage: Scenarios necessitating additional upper coverage, such as near exceptionally tall structures like skyscrapers, are relatively rare.
- 6. Complexity and Cost: The complexity and financial implications associated with implementing a six-sectoral plane system are substantial, necessitating considerable investments in both hardware and software integration.
- 7. High Operational Costs: Operational costs for such an expansive system would be significantly high, further burdening stakeholders involved in its deployment.
- 8. Maintenance Budget: A substantial budget would be required for ongoing maintenance to ensure long-term functionality and reliability, making the six-sectoral plane approach less viable in practical applications.

So, transitioning to a three-sectoral plane model will not only aligns with the principles of efficiency and effectiveness but also supports a more sustainable and economically feasible framework for the future of 3D-IRS technology.

The culmination of the 3D-IRS prototype development is illustrated in Figure 5, showcasing the final iteration of the design. This design results from a comprehensive analysis detailed in bullet points 1 through 8 of as listed previously. Ultimately, a triplanar configuration featuring three sides or faces was adopted, driven by the design's capacity to provide comprehensive spatial coverage, thereby enhancing wireless communication performance. The tri-planar structure optimizes the system's ability to manipulate electromagnetic waves across multiple planes, maximizing its potential to improve signal propagation and coverage in three-dimensional space. This final design synthesizes theoretical principles and practical considerations explored throughout the research, aiming to achieve full-space coverage in wireless communication systems suing Modified 3D-IRS apparatus to involve 3 sectors as shown in figure 4.

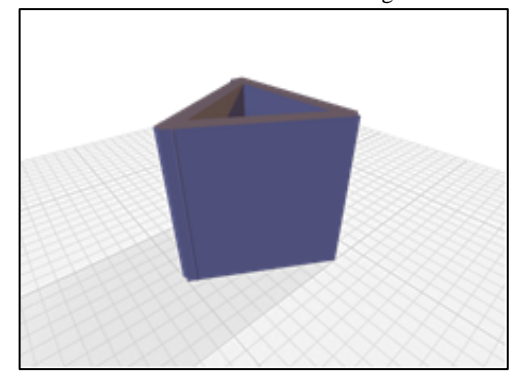


Figure 4 Modified 3D-IRS apparatus to involve 3 sectors

4. Coverage Maximization Algorithm **Improvement**

Investigating the Coverage Maximization Algorithm (CMA) [13] offers significant academic advantages, particularly in the evolving field of Reconfigurable Intelligent Surfaces (RIS), which are pivotal for modern wireless communication systems. The exploration of CMA's design, analytical frameworks, and optimization strategies opens new research opportunities, particularly in the context of enhancing network coverage—a critical concern for both current and future telecommunications networks. 3D-IRS is particularly relevant to CMA but in aspects of the advancement of 5G and emerging 6G technologies, addressing the pressing need for optimized coverage across diverse geographical landscapes. Its uniqueness lies in its emphasis on coverage area (m2) rather than traditional metrics like sum rate or throughput, making it a suitable algorithm for extending physical network coverage, especially in regions that are traditionally underserved.

CMA's methodological approach offers an optimal representation of network coverage by focusing on tangible, physical areas rather than abstract metrics, which is especially beneficial in densely populated urban environments where signal obstructions are common. The algorithm allows for practical enhancements in network performance by adjusting RIS placement, orientation, and phase shifts, resulting in improved signal coverage and user experiences. This focus on coverage-centric optimization is rare in contemporary research, which often prioritizes data rates and bandwidth allocation, creating a unique opportunity for further scholarly inquiry.

Moreover, the potential for future research on CMA is immense, as global demand for seamless connectivity increases. CMA's relevance extends to smart cities, rural connectivity, and vehicular networks, making it a fertile ground for future academic and industry-driven research. Additionally, CMA's accessibility makes it an appealing subject for individual scholars or small academic groups, as it does not require sophisticated equipment or largescale laboratories. The algorithm's practicality and scalability, ranging from indoor networks to large urban environments, further enhance its research appeal. CMA's system model focuses on optimizing the placement of a single IRS to maximize signal coverage, though it has limitations in reflecting signals in a single direction, which can lead to coverage gaps. In contrast, the 3D-IRS system model, designed for comprehensive cellular coverage, dynamically adjusts signal reflections across multiple dimensions and directions, overcoming physical obstructions and ensuring seamless coverage. This framework is particularly effective in dense urban settings, where obstacles frequently disrupt signals. The 3D-IRS framework's ability to continuously reconfigure and optimize coverage makes it a more robust solution compared to the one-directional CMA approach, ensuring higher quality of service (QoS).

A. System Visualization

The forthcoming diagram (Figure 5) illustrates the archetypal structure of IRS configuration. This visual representation serves as the cornerstone for understanding the integration of two key components within the system architecture: CMA and 3D-IRS framework. The schematic elucidates the fundamental elements and their interconnections, offering valuable insights into the spatial arrangement and functional relationships within the IRS setup.

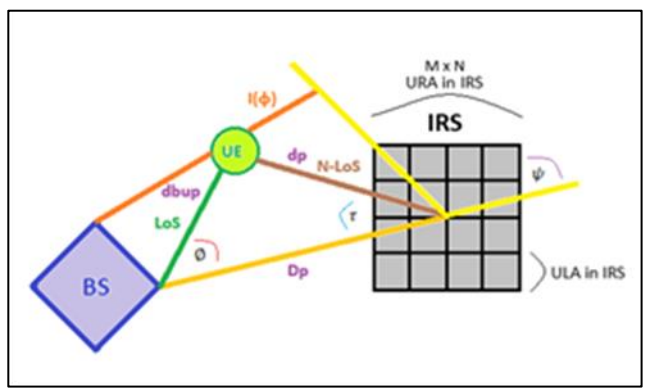


Figure 5 Structure of IRS

This depiction facilitates a comprehensive grasp of how the CMA operates in conjunction with the 3D-IRS to optimize coverage within the network. It visually contextualizes the algorithmic approach to maximizing signal propagation and reception through strategic manipulation of the intelligent reflecting elements in three-dimensional space.

B. Arithmetic calculation

Building upon the foundational concepts outlined in the CMA concept stated in the paper [18], this study identifies and derives key telecommunication parameters essential for further investigation. These parameters, drawn from a combination of academic sources and additional calculations, form the theoretical backbone of the research. By integrating established knowledge with contemporary advancements in telecommunications, the study enhances the depth and rigor of its analysis.

Further, the study acknowledges that foundational concepts in the IRS domain are often not repeated due to the abundance of existing literature, instead drawing on predefined parameters influenced by standardization efforts of the 3GPP organization [19] and other scholarly contributions such as [20].

First, it is crucial to calculate the real distances based on the plane distances using simply Pythagorean theorem, of course assuming all telecom nodes (BS, IRS, and UE) are on the same ground (i.e. base of all of them in the same level of the earth), finding the real distances d, D, and dbu which represent IRS-UE real distance as in equation (1), BS-IRS real distance as in equation (2), and BS-UE real distance as in equation (3) respectively.

$$d = \sqrt{dp^2 + (H_{IRS} - H_{UE})^2}$$
 (1)

$$D = \sqrt{Dp^2 + (H_{BS} - H_{IRS})^2}$$
 (2)

$$dbu = \sqrt{dbup^2 + (H_{BS} - H_{UE})^2}$$
 (3)

Where, dp, Dp, dbup HBS, HIRS, and HUE represent IRS-UE plane distance, BS-IRS plane distance, and BS-UE plane distance, Height of base station, Height of IRS, Height of UE (i.e. typical human length) respectively. Then, based on [21], the gain of channel in the N-LoS (i.e. Non Line of Sight) can be formulated simply to be using equation (4)

$$G_{N-LoS} = \frac{\lambda \times \sqrt{G_a \times S_M \times S_N}}{(4\pi)^{\frac{3}{2}} \times \sqrt{D_{(m,n)}^{\mu} d_{(m,n)}^{\mu}}} e^{-j\frac{2\pi}{\lambda}(D_{(m,n)} + d_{(m,n)})} \tag{4}$$

Where, GN-LoS, Ga, SM & SN, D(m,n), d(m,n), μ , and λ are representing gain of channel in the N-LoS, gain of antenna at BS, Single sub-modules in IRS size, real distance between BS and IRS in the (m, n)-th element for each beam, real distance between IRS and UE in the (m, n)-th element for each beam, and exponent of path-loss, and wavelength respectively.

Furthermore, to accurately determine the coverage area of the cell,

our analysis will centre on the identification of the cell edge, leading for the assumption that the UE is located within the far field region of the IRS, which allows us to establish the relationship d(m,n)=d, where d denotes the distance separating the UE from the centre of the IRS.

Consequently, this leads to the conclusion that the path loss incurred is consistent across all elements of the IRS, thereby highlighting the uniformity of the signal degradation experienced by the transmitted signals as they traverse the space between the IRS and the UE. This uniform path loss is critical for optimizing the performance of communication systems that leverage 3D-IRS technology, as it enables a more predictable analysis of the signal quality that can be anticipated by the UE.

To summarize, the spatial configuration and distances involved play a pivotal role in shaping the characteristics of the signal propagation, which ultimately influences the efficiency and effectiveness of the wireless communication network. Therefore, the assumptions made regarding the distances and their implications are fundamental to the theoretical framework that underpins the deployment and utilization of 3D-IRS in modern telecommunications like the sixth generation.

Thus, using the previous reference for obtaining MAX-SNR, tending to follow the after-mentioned strategy and making the formula distributed into three distinct values, namely SNR1, SNR2, and SNR3, for the sake of simplicity as in the following formulae (9), (10), and (11):

$$SNR1 = \frac{P_T \times \lambda^2 \times \cos^2(\tau) \times s_M \times s_N}{\sigma^2 \times (4\pi)^3}$$
 (9)

$$SNR2 = \frac{P_T \times \lambda^2 \times G_a}{\sigma^2 \times (4\pi)^2} \tag{10}$$

$$SNR3 = \frac{2 \times P_T \times \lambda^2 \times \sqrt{G_a} \times \cos(\tau) \times \sqrt{s_M \times s_N}}{\sigma^2 \times (4\pi)^{5/2}}$$
(11)

Now, knowing that from the unique scenario mentioned above, where equating the threshold SNR with the actual SNR (i.e. SNR=SNRth) result in very unique case in which d_{th} in respect to the angle ϕ is the same as dbup in this unique case. So by using [22], [23], let calculate the SNRth to be as following equation (12):

$$SNR_{th} = \rho \times \varepsilon = 28 \, dB + 8 \, dB = 36 \, dB \tag{12}$$

And, according to the findings presented in reference [24], the expression for the reflection coefficient pertaining to the specific (m, n)-th element in the IRS can be articulated in the following manner as the amplitude change (i.e. Å) can be expressed as in the following equation (13):

$$\mathring{A} = \frac{\Gamma_{m,n}}{e^{-j\varphi_{m,n}}} \tag{13}$$

Where, representing amplitude change, reflection coefficient, and phase shift respectively. It is presumed that the BS is positioned in the far field relative to the IRS. The variation in amplitude change denoted as Å, can be effectively modeled by employing the cosine function of the incidence angle, which is represented by the variable τ in this paper, that delineates the angle of incidence from the base station to the IRS.

Furthermore, it is postulated that the phase shift, denoted by (m, n)-th, remains unaffected by both the angles of incidence and reflection, thereby allowing for a simplified analysis of the system's behavior under these assumptions. This assumption is significant as it facilitates a clearer understanding of the interaction

dynamics between BS and IRS, while maintaining a focus on the essential parameters influencing the reflection characteristics of the (m, n)-th element within the broader context of wireless communication systems.

Then, from the previous equations, let calculate for dth in respect to the angle ϕ by following equation (14):

$$\zeta(\phi, d_{th}(\phi)) = SNR_{th}$$
 for all $\phi \in [0, 2\pi)$ (14)

Then, calculating for $\zeta(\phi, dbup)$ from will lead to the following overall formula (15):

$$\zeta(\phi, dbup) = SNR1 \times M^{2} \times N^{2} \times \left[\frac{G_{\alpha}}{D^{\mu}}(Dp - dbup \times \cos(\phi))^{2} + (dbup \times \sin(\phi))^{2} + (H_{IRS} - H_{UE})^{2}\right]^{\frac{-\mu}{2}} + \frac{SNR2}{(\sqrt{(dbup)^{2} + (H_{BS} - H_{UE})^{2}})^{2}} + SNR3 \times M^{2} \times N^{2} \times \frac{\sqrt{\left[\frac{G_{\alpha}}{D^{\mu}}(Dp - dbup \times \cos(\phi))^{2} + (dbup \times \sin(\phi))^{2} + (H_{IRS} - H_{UE})^{2}\right]^{\frac{-\mu}{2}}}{\sqrt{(dbup)^{2} + (H_{BS} - H_{UE})^{2}}}}$$
(15)

And by the same way as well, $I(\phi)$ can be obtained by the following equation (16):

$$I(\phi) = \frac{Dp}{\cos(\phi) - \sin(\phi) \times \cot(\phi)}$$
 (16)

So, overall system coverage is given by:

$$C_{IRS} = \int_{\phi l}^{\phi u} \frac{1}{2} d_{th}^{2}(\phi) d\phi + \frac{1}{2} sin(\phi l - \phi u) \times I(\phi u) \times I(\phi l)$$
 (17)

Where, ϕu is the upper angle and ϕl is lower angle.

That is,

Then, a proposed formula has been driven from the rule of segmentation of area. It is denoted by initials ASA as it represents Area of Segmental Arc, as shown in following equation (18)

$$ASA = \pi d_{th}^{2}(\phi) - \frac{1}{2} d_{th}^{2}(\phi) \times$$

$$(2 \times \arccos[\cos(\phi)] - \sin(2 \times \arccos[\cos(\phi)]))$$
[18)

RSSI (i.e. Received Signal Strength Indicator) measures the power of a received cellular signal, typically in dBm, and is crucial for assessing network performance [25]. In 3D-IRS, RSSI helps evaluate how effectively 3D-IRS enhances signal strength by reflecting signals to improve coverage, particularly in challenging environments.

C. Simulation parameters

The comprehensive investigation elucidates the significant role that both predetermined and calculated parameters, along with their associated symbols as defined by the upcoming table (Table 1), which act in facilitating a thorough comprehension of the system in question prior to the undertaking of more intricate and sophisticated analyses that may require a deeper level of understanding and insight. It is important to note that certain parameters are posited based on the specialized expertise and background knowledge possessed by the researchers involved in this study, while others are derived from fundamental reasoning or previous empirical investigations, and a number of key parameters are explicitly extracted from the CMA paper referenced as [13], establishing a vital link between the CMA and the 3D-IRS framework that emphasizes the shared mathematical principles and numerical values underpinning both methodological approaches. Additionally, the research acknowledges the reality that foundational concepts within the IRS domain are frequently not reiterated due to the substantial volume of existing academic literature; rather, the study opts to draw upon predetermined parameters that have been shaped by the standardization initiatives undertaken by the 3GPP organization, as indicated in reference [19], alongside other scholarly contributions, such as those denoted in reference [20]. For the sake of clarity and to facilitate understanding, the predefined parameters have been systematically organized and presented in Table 1, which serves as an essential reference point for the subsequent intricate and detailed calculations that are to follow in the course of this research.

Table 1: Overall Utilized Simulation Parameters in MATLAB

No#	Symbol	Value	Unit	Definition
1	С	299,792,458	m/s	Speed of light
2	M, N	25	none	Size of single IRS [Δ ULA]
3	H_{BS}	35	m	Height of base station
4	H_{IRS}	2	m	Height of IRS
5	H_{UE}	1.5	m	Height of UE (Human length)
6	σ^2	-96	dBm	Noise power
7	EIRP	42.3	dBm	Effective Isotropic Radiated Power
8	Ga	1	dBi	Antenna gain
9	Lcc	0	dB	Cables and connectors loss
10	μ	2	none	Exponent of path-loss
11	ε	8	dB	sensitivity of UE
12	ρ	28	dB	penetration loss margin
13	Ø	$[0, 2\pi)$	Radian	Angle between BS∠UE
14	ψ	$[0,\pi)$ Single	Radian	Angle between BS∠IRS
15	τ	$[0,\pi)$	Radian	Incidence angle BS∠IRS
16	dp	50	m	IRS-UE Plane distance
17	Dp	50	m	BS-IRS Plane distance
18	dbup	50 - 500	m	BS-UE Plane distance
19	λ	0.1	m	Wavelength
20	sN	0.04	m	Single sub-module in IRS size
21	sM	0.04	m	Single sub-module in IRS size
22	$\sigma^2 (dB)$	-126	dB	Noise power
23	$\sigma^2(W)$	2.5e - 13	W	Noise power
24	P_T	33.0103	dBm	Power of the transmitter
25	$P_T(W)$	2	W	Power of the transmitter
26	SNR_{th}	36	dB	Signal-to-noise ratio (threshold)
27	$SNR_{th}(W)$	4e + 3	W	Signal-to-noise ratio (threshold)
28	MN	625	none	Full size of complete IRS [URA]

5. Results and Discussion

This section presents and discusses the study's findings in relation to its goal of the research, which was to ascertain the impact of a full space coverage enhancement for cellular communication systems via three dimensional intelligent reflective surfaces via the use of MATLAB visual representations. The primary comparisons in assessing the impact of coverage area are based on two subscenarios: the first compares the acquisition of the algorithm through full integration coverage and without integration coverage, and the second is based on the situation/algorithm as show in Table 2.

Table 2: full space coverage enhancement comparison

Algorithem/situation	Coverage [No Integration]	Coverage [Full Integration]
BSS (1.5 W)	295060	N/A
Random (1.5 W)	452130	N/A
CMA	797680	N/A
ASA [Single IRS]	930200	N/A
3D-IRS [Two IRSs]	1307100	1583500
3D-IRS [Three IRSs]	1664300	1762300
Improvement of	In comparison to	Area and Percentage
Random	BSS	157070 [53.23 %]
CMA	Random	345550 [76.42 %]
ASA [Single IRS]	CMA	132520 [16.61 %]
3D-IRS [Two IRSs] - NI	ASA [Single IRS]	376900 [40.51 %]
3D-IRS [Two IRSs] - FI	3D-IRS [Two IRSs] - NI	276400 [21.14 %]
3D-IRS [Three IRSs] - NI	3D-IRS [Two IRSs] - FI	80800 [5.102 %]
3D-IRS [Three IRSs] - FI	3D-IRS [Three IRSs] - NI	98000 [5.888 %]

It becomes exceedingly pertinent to engage in a thorough discussion regarding the outcomes derived from the MATLAB simulations, as this analytical discourse is crucial for facilitating a comprehensive comparison between the two distinct systems or algorithms under scrutiny, namely the 3D-IRS and the CMA algorithm, thereby providing an expansive perspective on the enhancement of coverage and allowing for an in-depth examination of the variances observed in the behaviour of the respective curves when subjected to a variety of different parameters.

Upon the meticulous application of the simulation parameters outlined in previous Table 1, there emerges a distinctly clear visualization that becomes apparent, revealing a significant margin of improvement in terms of cellular coverage, particularly when the singular Intelligent Reflecting Surface was subjected to rigorous testing, in contrast to the multiple Intelligent Reflecting Surfaces integrated within the framework of the 3D-IRS system, thereby highlighting the efficacy of these advanced technologies in enhancing coverage.

There has been a noteworthy enhancement regarding the threshold distance, which can be quantified by the calculation (345 - 306 =39 meters), as vividly depicted in Figure 6, particularly when employing a constant base station transmitted power of 2 Watts, thereby indicating a significant advancement in operational efficiency.

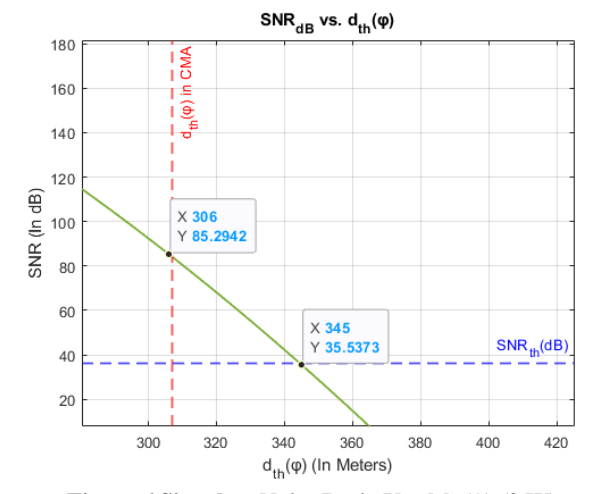


Figure 6 Signal-to-Noise Ratio Vs. dth (φ) (2 W)

Furthermore, the overall coverage area that can be achieved between the two distinct systems has been calculated to be (930200 -797680 = 132520 m2) by integrating the both algorithms and finding the area under the curve, which represents the total spatial area available for cellular coverage, and this is meticulously illustrated in Figure 7 for clearer understanding of the spatial dynamics involved.

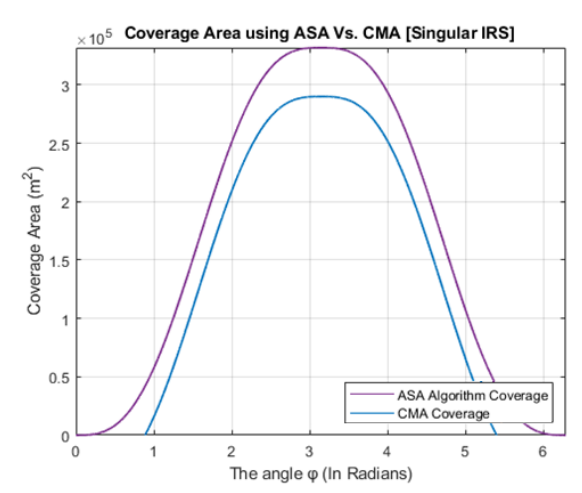


Figure 7 Coverage Area using ASA vs. CMA in Single IRS (2W)

In Figure 8, the distance denoted as $I(\varphi)$, which is utilized for

determining both the upper and lower calculated angles, is prominently featured within the aforementioned figure, and it becomes evident that the line where these two angles intersect shall be designated as the pivotal line that facilitates the handover process to the subsequent IRS.

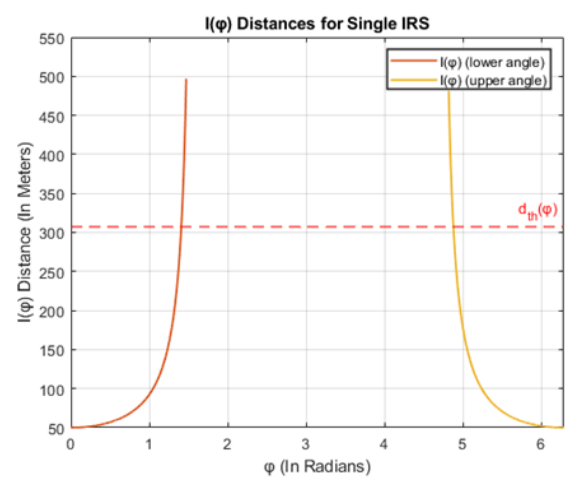


Figure 8 Distances for Single IRS (2 W)

Transitioning to a particularly intriguing aspect of this research, delving into the determination of the comprehensive 3D-IRS coverage throughout the entirety of the spatial volume, using two IRSs as represented in Figure 10, where the red intersecting lines symbolize the constraints imposed by the CMA, while the green lines depict the same 3D-IRS coverage scenario but without accounting for the complexities of system, as shown in Figure 9.

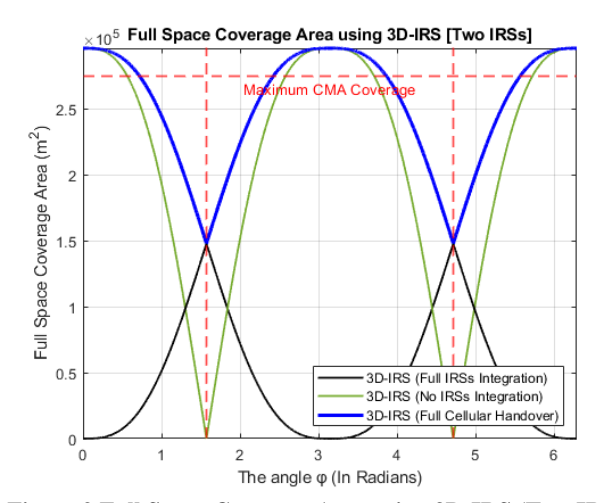


Figure 9 Full Space Coverage Area using 3D-IRS (Two IRSs)

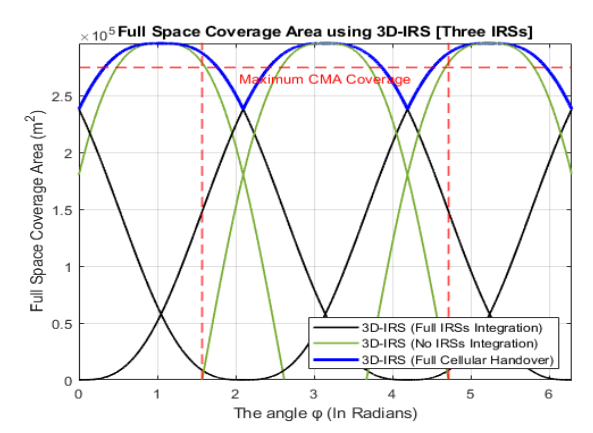


Figure 10 Full Space Coverage Area using 3D-IRS (Three IRSs)

Now, turning the attention to the diagram that represents the 3D-IRS, it becomes evident that this illustration serves as a pivotal focal point of the 3D-IRS framework and encapsulates the primary objective of this research, which is fundamentally aimed at significantly enhancing spatial coverage for cellular communication systems through the strategic implementation of using three intelligent reflective surfaces, utilizing a tri-planar configuration of IRSs to attain comprehensive advantages in terms of area coverage, as precisely shown in Figure 10

Subsequently, in Figures 11 and 12, there is a detailed representation of the Received Signal Strength Indicator (RSSI) values in relation to the total count of the elements' sizes, specifically indicated as (i.e. M^2 or N^2), as well as the varying distances measured between the base station and the intelligent reflecting surface, respectively, thus providing a comprehensive overview of the interaction between these critical parameters in the context of wireless communication systems.

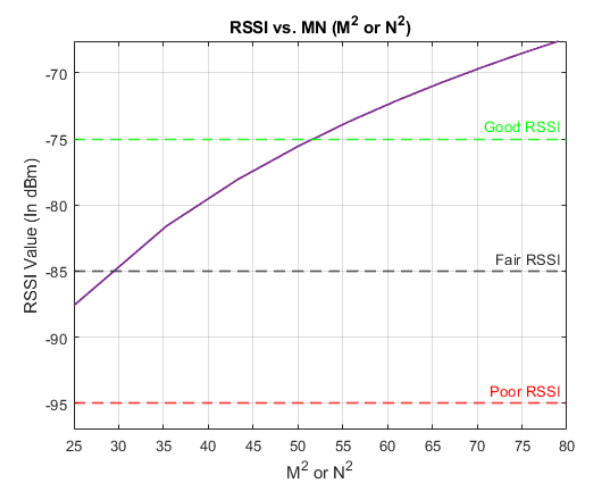


Figure 11 RSSI value in dBm Vs. M*N

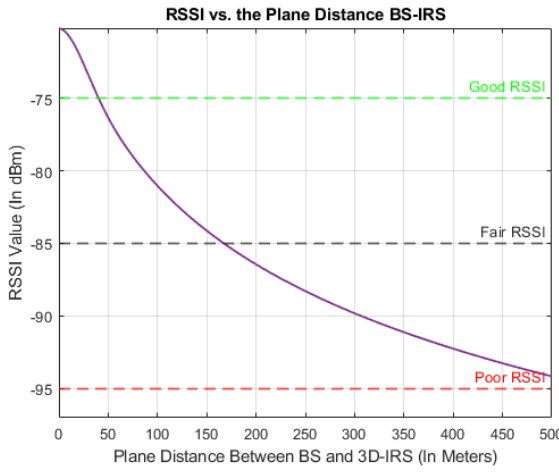


Figure 12 RSSI value in dBm Vs. BS-IRS distance

6. Conclusion

This MSc research shows the substantial advantages of 3D-IRS in enhancing cellular coverage and network efficacy in the full space spatial horizon and significantly advances the understanding of 3D-IRS technology's role in wireless communications. The efficacy of 3D-IRS has been demonstrated in enhancing cellular coverage compared to traditional IRS/RIS. The research indicates significant improvements in both threshold distance (m) and overall coverage area (m²) when compared with the CMA study. In singular IRS configurations, with a BS power of 2 Watts, the

threshold distance increased by 39 meters, while the coverage area expanded by 132520 m2. Two IRSs deployments yielded even more coverage of 1583500 m² when applying for the IRSs full integration. Finally, three IRSs contraption lead to have a substantial covered area of 1762300 m² when using all of the integrated planners. Additionally, the analysis of RSSI indicated that 3D-IRS maintained superior signal quality over increased distances, particularly influenced by the number of reflective elements and the base station transmitting power. Notably, the potential for improved handover mechanisms was identified, enhancing accuracy and reliability in NW performance.

References

- [1] X. Shao et al., "Target sensing with intelligent reflecting surface: Architecture and performance," IEEE J. Sel. Areas Commun., vol. 40, no. 7, pp. 2070-2084, 2022.
- [2] M. Di Renzo et al., "Smart radio environments empowered by reconfigurable intelligent surfaces: How it works, state of research, and the road ahead," IEEE J. Sel. Areas Commun., vol. 38, no. 11, pp. 2450-2525, Nov. 2020.
- [3] Q. Wu and R. Zhang, "Beamforming optimization for wireless network aided by intelligent reflecting surface with discrete phase shifts," IEEE Trans. Commun., vol. 68, no. 3, pp. 1838-1851, Mar.
- [4] Q. Wu and R. Zhang, "Towards smart and reconfigurable environment: Intelligent reflecting surface aided wireless network," IEEE Commun. Mag., vol. 58, no. 1, pp. 106-112, Jan.
- [5] H. Li et al., "Reconfigurable Intelligent Surfaces 2.0: Beyond diagonal phase shift matrices," arXiv preprint arXiv:2301.03288, 2023.
- [6] H. Shen, B. Clerckx, and R. Murch, "Modeling and architecture design of reconfigurable intelligent surfaces using scattering parameter network analysis," IEEE Trans. Wireless Commun., vol. 21, no. 2, pp. 1229-1243, 2021.
- [7] F. Liu, D. Kwon, and S. Tretyakov, "Reflectarrays and metasurface reflectors as diffraction gratings: A tutorial," IEEE Antennas Propag. Mag., vol. 65, no. 3, pp. 21-32, 2023.
- [8] Y. Guo et al., "Joint beamforming for RIS aided full-duplex integrated sensing and uplink communication," in Proc. IEEE Int. Conf. Commun. (ICC), 2023.
- [9] Y. Liu et al., "Beamforming design and performance evaluation for reconfigurable intelligent surface assisted wireless communication systems with non-ideal hardware," arXiv preprint arXiv:2006.00664, 2020.
- [10] V. K. Chapala and S. M. Zafaruddin, "Multihop RIS-assisted FSO-RF system over double generalized gamma fading," arXiv preprint arXiv:2108.07236, 2021.
- [11] R. Xiong et al., "Design of reconfigurable intelligent surfaces for wireless communication: A review," arXiv preprint arXiv:2304.14232, 2023.
- [12] Q. Sultan et al., "Fast beam training technique for millimeterwave cellular systems with an intelligent reflective surface," Sensors, vol. 21, no. 14, p. 4936, 2021.
- [13] S. Zeng et al., "Reconfigurable intelligent surface (RIS) assisted wireless coverage extension: RIS orientation and location optimization," IEEE Commun. Lett., vol. 25, no. 1, pp. 269-273, 2020.
- [14] H. Li, S. Shen, and B. Clerckx, "A dynamic grouping strategy for beyond diagonal reconfigurable intelligent surfaces with hybrid transmitting and reflecting mode," IEEE Trans. Veh. Technol., vol. 72, no. 12, pp. 16748-16753, 2023.

- [15] A. Rech et al., "Downlink TDMA scheduling for IRS-aided communications with block-static constraints," 2023.
- [16] X. Qian et al., "Joint optimization of reconfigurable intelligent surfaces and dynamic metasurface antennas for massive MIMO communications," in Proc. IEEE 12th Sensor Array Multichannel Signal Process. Workshop (SAM), 2022.
- [17] R. J. Williams et al., "Electromagnetic based communication model for dynamic metasurface antennas," IEEE Trans. Wireless Commun., vol. 21, no. 10, pp. 8616-8630, 2022.
- [18] M. Rossanese et al., "Designing, building, and characterizing RF switch-based reconfigurable intelligent surfaces," in Proc. 16th ACM Workshop Wireless Netw. Testbeds, Experimental Eval. CHaracterization, 2022.
- [19] 3GPP, "Study on channel model for frequencies from 0.5 to 100 GHz (Release 14)," 3GPP TR 38.901, Jan. 2018.
- [20] B. Di, H. Zhang, L. Song, Y. Li, Z. Han, and H. V. Poor, "Hybrid beamforming for reconfigurable intelligent surface based multi-user communications: Achievable rates with limited discrete phase shifts," IEEE J. Sel. Areas Commun., vol. 38, no. 8, pp. 1809-1822, Aug. 2020.
- [21] H. Zhang, B. Di, L. Song, and Z. Han, "Reconfigurable intelligent surfaces assisted communications with limited phase shifts: How many phase shifts are enough?" IEEE Trans. Veh. Technol., vol. 69, no. 4, pp. 4498-4502, Feb. 2020.
- [22] J. Thornton, D. Grace, M. H. Capstick, and T. C. Tozer, "Optimizing an array of antennas for cellular coverage from a high altitude platform," IEEE Trans. Wireless Commun., vol. 2, no. 3, pp. 484-492, May 2003.
- [23] H. Wang, P. Zhang, J. Li, and X. You, "Radio propagation and wireless coverage of LSAA-based 5G millimeter-wave mobile communication systems," China Commun., vol. 16, no. 5, pp. 1-18, June 2019.
- [24] Ö. Özdogan, E. Björnson, and E. G. Larsson, "Intelligent reflecting surfaces: Physics, propagation, and pathloss modeling," IEEE Wireless Commun. Lett., vol. 9, no. 5, pp. 581-585, 2019.
- [25] L. Polak et al., "Measurement and analysis of 4G/5G mobile signal coverage in a heavy industry environment," Sensors, vol. 24, no. 8, p. 2538, 2024.